NEAR ZERO-POWER ENVIRONMENT TEMPERATURE MICROMECHANICAL SENSOR-SWITCH ENABLED BY SUB-MICRON GAP

Duan Jian Goh[1], *Yul Koh*[1], *Sagnik Ghosh*[1], *Jaibir Sharma*[1], *Yong Shun Teo*[1], *Amit Lal*[2], *and Joshua E.Y. Lee*[1]

[1]Institute of Microelectronics, Agency for Science, Technology and Research (A-STAR), SINGAPORE and

[2]Cornell University, USA

ABSTRACT

In this work, we present a novel zero-power cantilever type temperature sensor-switch with a sub-micron (~700nm) contact gap. The sub-micron gap enables the device to switch on at just 10°C above room temperature for environmental temperature sensing. The device comprises a bimorph cantilever comprising Silicon (Si) and Aluminum (Al), with Titanium Nitride (TiN) switch contacts at the free end. We successfully demonstrate switch activation at 35°C, drawing an on-state power of <3µW while consuming near zero-power in the off-state. The device could be applied to monitor food storage temperatures where the sensor, as part of a wireless sensor node, is triggered when the room temperature goes above the warning level but draws nearly zero-power otherwise.

KEYWORDS

Near zero-power sensors, MEMS switch, temperature sensors, bimorph, cantilever.

INTRODUCTION

With rising deployment of Internet of Things (IoT), wireless temperature monitoring is one of the most important applications [1]. In terms of implementation, these IoT temperature sensors hold a broad range of applications spanning manufacturing to agriculture, IoT sensors enable interconnection between analog-to-digital platforms, harvesting environmental data in IoT networks [2]. Currently, temperature sensing has largely relied on band-gap temperature sensors and thermistors which continuously consume around 1µW power. As such, batteries from sensor nodes discharge within several months, which remains a bottleneck for massive deployment of IoT sensors. With the aim to reduce power consumption, concepts of zero-power MEMS switches has proposed in previous works, showcasing low power consumption requirements to deliver event-based switching operations [3] [4].

In this work, we introduce the concept of a near zero-power MEMS temperature switch which is applied here to environment temperature (<40°C) sensing for the first time. The intrinsic mechanical deformation behavior of cantilevers has found advantages for application in this work. Under temperature change, the MEMS temperature switch operates with a cantilever beam which is responsive within a targeted temperature range. Design of the device has focused on producing reliable switching operations through the contact layers.

We document the full switching process during thermal cycling, illustrating the capability of the switch attaining low power switching from a direct power supply voltage of 3V.

TEMPERATURE SENSOR-SWITCH DESIGN AND FABRICATION

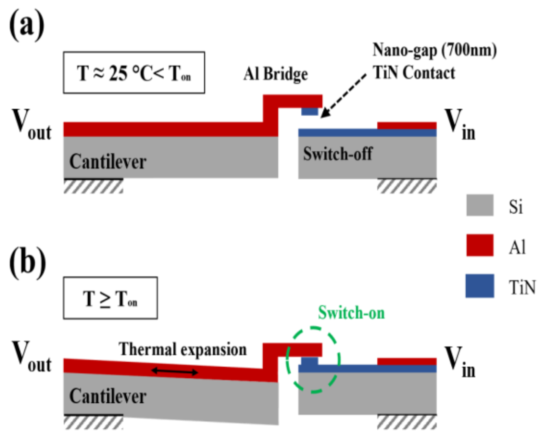

Figure 1: Cross sectional schematic of the sub-micron gap temperature switch depicting its working principle; (a) switch in the off state at $T < T_{on}$ and (b) turned on at $T > T_{on}$ due that thermal expansion of Al is larger than Si.

A. Operation Principle

The principle of the proposed MEMS temperature switch is based on the deflection of an Al-Si bimorph cantilever due to differentiated thermal expansion of its constituent layers. Fig 1 illustrates the working principle of the device, based on an Al-Si bimorph cantilever. The main mechanism for switching occurs at the tip of the cantilever formed by an Al bridge with TiN contacts. At room temperature when the device is in the off state, the Al bridge is initially separated from the counter electrode (Fig. 1a). Increasing temperature causes the cantilever to bend downward due to the larger thermal expansion coefficient of Al over Si (TCE: Al= 23.1ppm/K, Si=2.6ppm/K). The contacts close when the ambient temperature T is above the turn-on threshold temperature (T_{on}) (Fig. 1b). T_{on} can be reduced by either making the cantilever longer for a more compliant structure, or by narrowing the gap to close the switch with a smaller deflection. The sub-micron gap contact structure used in this work enables us to reduce T_{on} to 35°C.

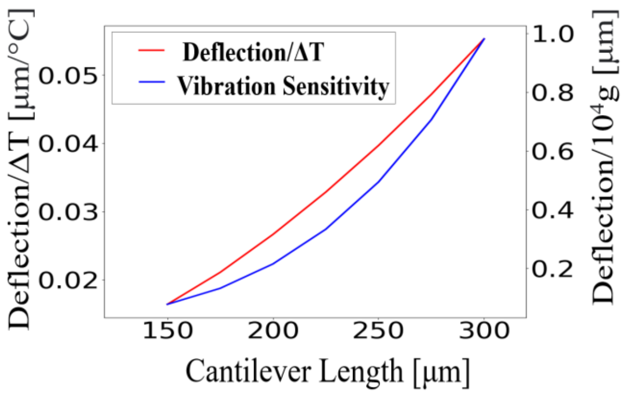

Figure 2: FE simulation for a comparison of thermal vs. vibration sensitivity as a function of cantilever length.

B. Simulation Results

COMSOL finite element (FE) simulations were performed to study the temperature sensitivities and vibration sensitivities as a function of cantilever lengths in the range of 150μm to 300μm. As shown in Fig. 2, the temperature sensitivity (μm/°C) was found to increase almost linearly with increasing cantilever length. The simulation result also compares the tip displacement (based on a 5μm-thick silicon layer) with respect to a 1°C rise vs. 10^4g (high g-shock) acceleration. Within this analysis, longer cantilevers were found to be more sensitive to vibrations with sensitivity exponentially increased with cantilever length. Therefore, there is a design challenge of reducing T_{on} to lie within 35°C while having low sensitivity to vibration. An optimum solution was chosen by designing for a shorter cantilever, for which the higher stiffness is compensated by a narrower contact gap in order to maintain a lower sensitivity to vibrational shock [5]. In addition, the FE simulation result verified that lowering T_{on} to within 10°C above room temperature was possible using a sub-micron contact gap for the chosen design.

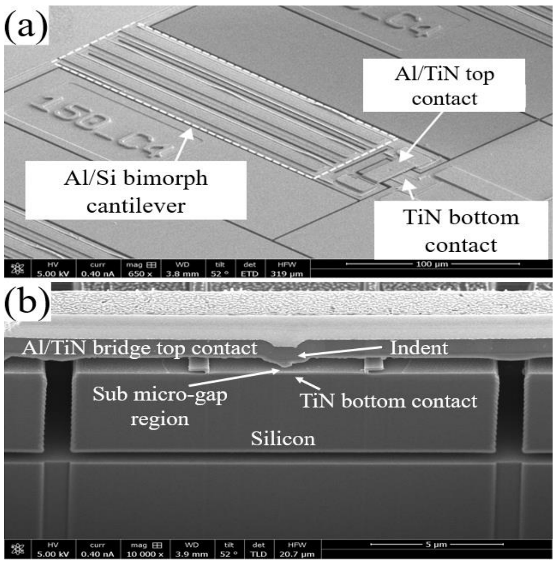

Figure 3: SEM image of fabricated nano-gap cantilever temperature switch; (a) Perspective view of the device and (b) FIB-cut cross-sectional image for the sub-micron gap contact and supporting cantilever.

C. Fabrication Results

The presented MEMS temperature switch was fabricated using IME's sensor-switch process [6]. The devices were fabricated using 5μm SOI (Silicon-On-Insulator) wafers with a SiO_2 box layer of 1μm. The detailed flow of this fabrication process has been reported previously in [7]. Fig. 3(a) shows the overall image of the cantilever taken under Scanning Electron Microscopy (SEM). The Al/Si bimorph cantilever features a single fixed end beam, with an Al/TiN top contact bridge contact positioned at the tip of the cantilever's free end. The bridge contains an indent (Fig. 3(b)) to minimize the contact area with the aim to improve reliability by mitigating against stiction. The gap between the tip of the indent and the bottom electrode is about 700nm. Fig 3(b) shows the cross-section of the sub-micron contact gap under Focus Ion Beam (FIB) analysis. The cross-section image reveals an indent profile of (2μm x 2μm x 0.3μm) underneath the Al/Si during FIB. Directly between the indent and TiN bottom contacts, the sub-micron region can also be clearly seen. The purpose of the indent pattern is to provide additional depth to promote the electrical contact between top Al electrode and the bottom TiN contact. It was formed prior to a SiO_2 etch where a mold was created for indent formation. During Al patterning stage, Al is deposited to fill the mold cavity forming the resulting indent profile. Besides being the main medium for electrical contact bridging, it is an additional design feature to minimize electrical contact stiction effects as reported in [8]. This results in an indent size where its dimension is kept minimal to process design requirements.

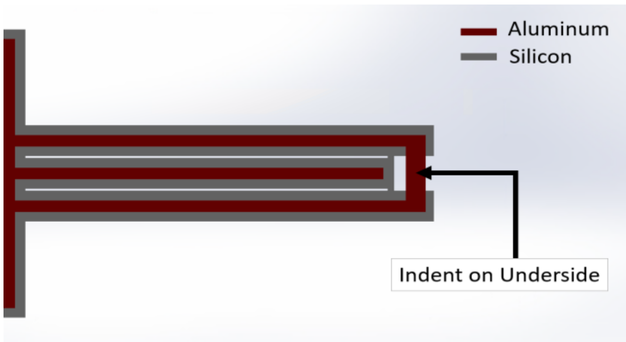

Figure 4: Top-View image of segmented cantilever design in SolidWorks

The key feature of the device cantilever design is the 3-segmented cantilevers conjoined together as shown in Fig. 4. During the design phase, the cantilever width was kept within ~12μm to achieve better device sensitivity. Another consideration in the design was the reduction of lateral deflection during the thermal switching process. Subsequent design iterations resulted at the presented concept, where the introduction of accompanying side cantilevers seeks to reduce the effects of lateral deflection during the switching operation of the device. Cantilever lengths of 150μm and 275μm lengths were fabricated, and the respective experimental results compared in the next section.

EXPERIMENTAL RESULTS

For switching evaluation, two phases of experiments were carried out for validation of the device's performance. First, an experiment was conducted to correlate the thermal deflection and electrical contact signal of the switch using the 150µm long cantilever as the test device. Temperature sweeps (ramp up and ramp down) were applied to the device with optical deflection and switch output monitored concurrently. Next, temperature cycling tests were conducted to evaluate the electrical switching performance with environment temperature change using the 150µm and 275µm long cantilevers switches for comparison.

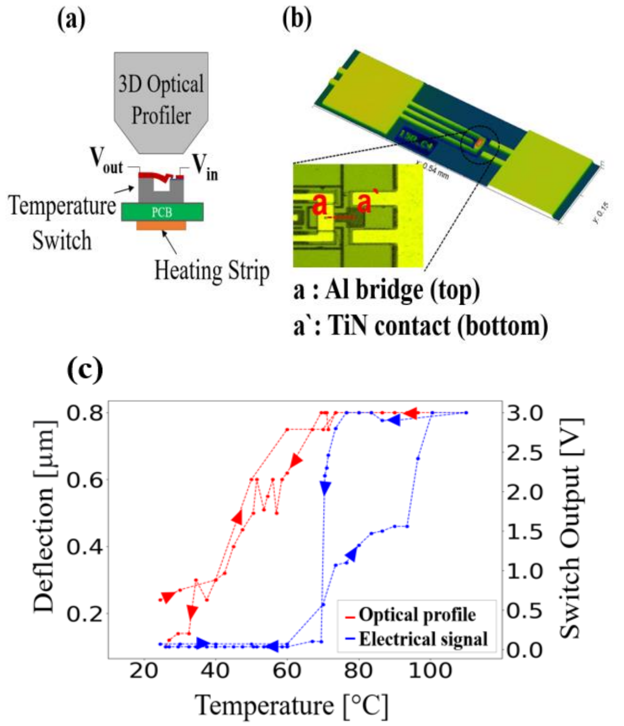

Figure 5: Measurements for correlating tip deflection and switch electrical output in response to thermal ramp up and down. (a) Experiment setup, (b) 3D profile acquired by optical profiler, (c) Cantilever tip deflection against contact output across section a-a' indicated in (b).

A. Correlation of thermal deflection and electrical contact signal of the sensor-switch

The fabricated devices were diced and die-attached onto custom-designed printed circuit boards (PCBs). Subsequently, the dies were wire bonded at close to ambient temperature for better control of environmental factors induced on the cantilevers before the experiment. To examine the thermal response of the temperature sensor-switch in relation to the contact mechanics, we first obtained the surface profile of a 150µm-long bimorph cantilever during a thermal ramping up/down sequence. As shown in Fig. 5a and b, heat was applied to the device by attaching a polyimide heater strip on the underside of the PCB to control the temperature of the chip. A 3V bias was supplied through a DC power supply to the Al bridge via a bonded contact pad. The output signal from the switching event was captured on an oscilloscope (Keysight DSOX3034T) to measure the electrical response simultaneously while the optical profile was acquired. The tip deflection and voltage output are plotted in Fig. 5c. A platinum resistance temperature detector (Pt RTD) was attached on the PCB surface for tracking of the actual temperature during the temperature sweep process. The RTD is further wired to a digital tabletop multimeter for resistance readout. The resistance values were subsequently converted to temperature values provided from the RTD's product manual.

During thermal ramp up, profile deflection and electrical responses were captured simultaneously. Within the anticipated range for T_{on} / T_{off} switching events, both profile deflection data and switch contact output were acquired at 3°C step intervals. The temperature stabilization time was ~2 minutes for each step. Deflection of the cantilever tip plateaued around 70°C, indicating micron gap closure (deflection of ~0.8µm) between the Al bridge and TiN bottom electrodes on the cantilever surface. From this point, the output voltage begins to rise with the increase in contact force with further increase in temperature. Beyond this point, the gradual increase in contact switch output is indicative of the increasing electrostatic pull-in force generated, which gradually enhances the interfacial micro contacts between the top and bottom electrodes of the switch. Full electrical contact was established at around 100°C and maintained until 110°C,where the contact output voltage was maintained at the same level as the input voltage of 3V. In the next phase, voltage supplied to the polyimide strip was gradually reduced for the temperature ramp down sequence to begin. It could be observed that detachment occurs at ~70°C where contact was first established in the preceding ramp up sequence. At the point where the switch contact output reduced to ~2.2V, a drastic drop in contact output occurred with the profile and electrical data points during this phase within a narrow interval of ~0.5°C. The optical deflection profile was maintained at ~0.8µm when the switch contact output drops to ~100mV, indicating interfacial loss of electrical contact at the micro level between Al and TiN contact surfaces. With further temperature ramp down, the cantilever tip deflection was gradually restored to ~0.2 µm at ~25°C, within the initial range of cantilever deflection at the beginning of the experiment. As such, by superimposing of the optical profile deflection and electrical switching response of the cantilever, we can see that electrical contact is established and broken between 70°C to 100°C for this cantilever.

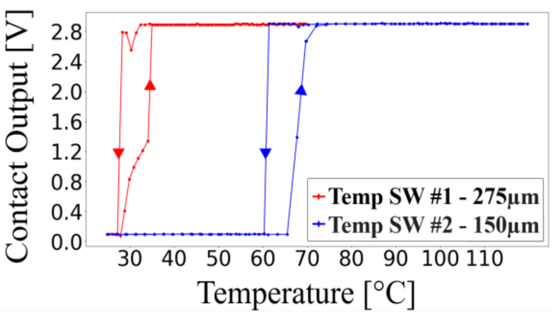

Figure 6: Temperature cycling test results for Temp SW #1 (longer cantilever with length of 275µm targeting turn on at around 35°C) and Temp SW #2 (shorter reference cantilever with length of 150 µm) that shows a distinctly higher turn on temperature.

B. Temperature Cycling Test

In the later experiment, the same cantilever (with a length of 150µm) along with a separate 275µm device was tested in a temperature chamber (ESPEC SH-242) for monitoring of its the electrical output. Both devices were subjected to temperature sweeps within the chamber to simulate environmental temperature change conditions. As with the previous experiment, a voltage of 3V was supplied from an external DC power supply through an SMA cable to bias the Al bridge of the switch for each device. The contact signals from the devices were monitored on an oscilloscope with a load of 1MΩ. In this set of experiments, the measured DC value from the oscilloscope was acquired with temperature swept between 25°C and 120°C. An additional Pt RTD was placed within the chamber to ensure the reliability of the temperature measured by the chamber's internal temperature sensor. The resistance values were converted to temperature values in a similar method as described for the previous experiment. The temperature difference between the RTD and chamber measured temperature was within 1~2°C. The temperature sweeping process was fully automated through python communication with oscilloscope readings taken at 1°C increments. At the various temperature points, the settling time was set for temperatures to fall within a 1°C tolerance prior to data acquisition. Next, the switch output voltages were acquired and saved into a data array for processing.

As shown in Fig. 6, the shorter switch (Temp SW #2) of 150µm turns on at a distinctly higher temperature of 67°C compared to the longer switch (Temp SW #1) of 275µm which switched on at 35°C if the threshold voltage is set to 1.2V. The accuracy of the switch on temperature is within ± 1°C based on the sharp transition.

C. Experiment Methodology Comparison

Compared to the optical profiler experiments discussed in the previous section, the data obtained from testing in the temperature-controlled chamber yielded a more well-defined switching cycle. Ambient conditions played a huge contribution in these set of experiments. The method of heat application also makes a distinctive difference: using a polyimide heating strip with the device is exposed to the ambient vs. a testing chamber where the temperature is well controlled. In the case of heating via a heating strip attached under device test PCB, the air region surrounding the device remains in ambient condition (~25°C) in a typical laboratory setting. Heat from the polyimide strip travels upwards through the PCB via conduction for thermal transfer. While the reference Pt RTD on the PCB monitors the temperature of the PCB, convection effects around the chip cannot be monitored. These uncertainties are avoided by carrying out the experiment in an enclosed temperature chamber. The switching temperatures noted from the experiments in the chamber are supported by the simulation results. In both cases, the presented cantilever designs were able to attain a temperature difference between T_{on} and T_{off} within ~10°C.

CONCLUSION

In this paper, we have successfully demonstrated temperature sensor switches activated at an environment temperature as low as 35°C for the first time. As a wake-up sensor for IoTs, the temperature sensor switch does not consume power until the detection of an event, namely the rise of the environment temperature above T_{on} of 35°C. The design balances the need to reduce vibration sensitivity while maintaining a sufficient temperature sensitivity to enable switching at such small difference from room temperature by realizing a sub-micron contract gap in the switch. We show that T_{on} can be tuned according to the length of the bimorph cantilever in accordance with the simulation results. In terms of hysteresis, the difference between T_{on} and T_{off} is kept within 10°C. In summary, deployment of such environmental sensing switch could provide a pathway towards near zero-power consumption and extension of battery life to unattended wireless sensing nodes.

ACKNOWLEDGEMENTS

This research work was supported by A*STAR under "Nanosystems at the Edge" programme (Grant number: A18A4b0055)

REFERENCES

[1] S. Villamil, C. Hernández, and G. Tarazona, "An Overview of Internet of Things", *Telkomnika (Telecommunication Comput. Electron. Control.)*, vol. 18, no. 5, pp. 2320–2327, 2020.

[2] C. Perera et al., "Sensor Search Techniques for Sensing as a Service Architecture for the Internet of Things", in *IEEE Sensors Journal*, vol. 14, no. 2, pp. 406-420, Feb. 2014.

[3] S. Ghosh et al., "Wake-Up IoT Wireless Sensing Node Based On A Low-G Threshold MEMS Intertial Switch With Reliable Contacts", in *Digest Tech. Papers IEEE MEMS'23 Conference,* Munich, Germany, January 15-19, 2023.

[4] R. H. Olsson, C. Gordon, and R. Bogoslovov, "Zero and Near Zero Power Intelligent Microsystems," *J. Phys. Conf. Ser.*, vol. 1407, 2019.

[5] C. L. Cheng, M. H. Tsai, and W. Fang, "Determining the Thermal Expansion Coefficient of Thin Films for a CMOS MEMS Process Using Test Cantilevers", *J. Micromech. Microeng*., vol. 25, no. 2, 2015.

[6] S. Merugu, et al., "A Novel Fabrication Platform for Acceleration Sensor Switch with Top Contacts," *2021 21st International Conference on Solid-State Sensors, Actuators and Microsystems (Transducers),* June 20-25, 2021.

[7] Y. Koh et al., "Nano-Gap Contact MEMS Torsional Mode Acceleration Switch Wake-Up Sensor", in *Digest Tech. Papers IEEE SENSORS'22 Conference*, Texas, USA, October 30 – November 2, 2022.

[8] B. Bhushan et al., "AFM Study of Perfluoroalkylsilane and Alkylsilane Self-Assembled Monolayers for Anti-Stiction in MEMS/NEMS", *Ultramicroscopy*, vol. 105, issues 1–4, 2005.

CONTACT

*D. J. Goh; Goh_Duan_Jian@ime.a-star.edu.sg